Optics Letters

Generation of coherent extreme ultraviolet radiation from α–quartz using 50 fs laser pulses at a 1030 nm wavelength and high repetition rates

Tran Trung Luu,[1,*] Valerio Scagnoli,[2,3] Susmita Saha,[2,3] Laura J. Heyderman,[2,3] and Hans Jakob Wörner[1]

[1]Laboratorium für Physikalische Chemie, ETH Zürich, Vladimir-Prelog-Weg 2, 8093 Zürich, Switzerland
[2]Laboratory for Mesoscopic Systems, Department of Materials, ETH Zürich, 8093 Zürich, Switzerland
[3]Laboratory for Multiscale Materials Experiments, Paul Scherrer Institute, 5232 Villigen PSI, Switzerland
*Corresponding author: trung.luu@phys.chem.ethz.ch

Received 17 January 2018; revised 20 February 2018; accepted 2 March 2018; posted 5 March 2018 (Doc. ID 319623); published 10 April 2018

Coherent extreme ultraviolet (EUV) radiation using high-harmonic generation (HHG) in *α*–quartz is demonstrated from 10 to 200 kHz, using 50 fs laser pulses at the center wavelength of 1030 nm. The EUV radiation extends beyond 25 eV in the nondamaging regime. The number of photons generated in a single harmonic order at 15.6 eV is measured to be $\approx(3.5 \pm 2.5) \times 10^{10}$ per second which, to the best of our knowledge, is a first and record value reported to date using EUV HHG from solids. This Letter demonstrates one of the first *all-solid-state* EUV sources based on industrial-grade fiber lasers, enabling the possibility of bringing reliable EUV sources to the mass market.

OCIS codes: (320.0320) Ultrafast optics; (140.0140) Lasers and laser optics.

https://doi.org/10.1364/OL.43.001790

Attosecond science [1,2], the study of electronic dynamics on their natural time scales, stems from the development of mostly extreme ultraviolet (EUV) sources through high-order harmonic generation (HHG) in the gas phase [3,4]. Recently, HHG in solids has been discovered [5], and it has quickly become the topic of active research with reports covering many different solid materials [6–13], solid structures [10,12,14], and spectral ranges [5–7,11]. Although the main physical mechanisms underlying HHG from solids are interband and intraband excitations, the interplay between them is a topic of active discussion at the moment [6,7,9,10,15–19]. Moreover, the emitted radiation [20] can be readily used for applications such as to initiate charge dynamics in molecules [21,22]. Being a promising source, EUV HHG from solids has so far been limited to using either short laser pulses [7,13] or low repetition rates (3 kHz) [7].

In this Letter, we explore the possibility of generating EUV HHG from solids using less stringent laser pulse characteristics that are more broadly available, particularly from the extremely reliable and increasingly popular fiber lasers. We demonstrate that EUV HHG can still be generated using much longer laser pulses. Furthermore, the frequency of the EUV HHG can be scaled up by two orders of magnitude (200 kHz) with only a slight drop of spectral intensity or photon flux per laser shot and, therefore, a massive gain of photon flux per unit time. Additionally, due to the nature of solid samples, which possess negligible vacuum evaporation, HHG of solids eliminates the need for turbo–molecular pumps that are required in HHG from gases. Therefore, the experimental apparatus can be made extremely compact: our HHG solids chamber has the footprint of 5 × 5 × 30 cm.

The chosen laser system is a commercially available ultrashort fiber amplifier (Active Fiber Systems). The amplifier delivers laser pulses at the center wavelength of 1030 nm, and the spectral bandwidth is 34 nm at full width at half-maximum. The pulse energy can be up to 50 μJ, and the collimated beam size is 2.9 mm measured at $1/e^2$. Most importantly, the repetition rate can be computer controlled in the range 6 Hz –200 kHz. The pulse duration is measured and optimized using a transient grating frequency resolved optical gating [23] apparatus. For all the repetition rates used in this Letter, the pulse duration does not change; it is maintained at 50 fs. Thanks to the low dispersion of air and glass in this spectral range, the duration of the pulses arriving on the sample is precisely the duration we measured outside vacuum.

In the experimental setup shown in Fig. 1(a), the laser pulses are focused ($f/50$) on the z-cut *α*–quartz crystal with a thickness of ∼20 μm, which was chosen for two reasons. First, knowing that thinner crystals lead to higher cutoff energy, we chose crystalline *α*–quartz which is mechanically strong and is the thinnest commercially available, compared to other types of SiO_2. Second, because it is noncentrosymmetric, crystalline *α*–quartz allows the generation of even harmonics which offers more possibilities for applications. The resultant emission is recorded downstream using a flat-field EUV spectrometer consisting of a grating and a multichannel-plate (MCP)

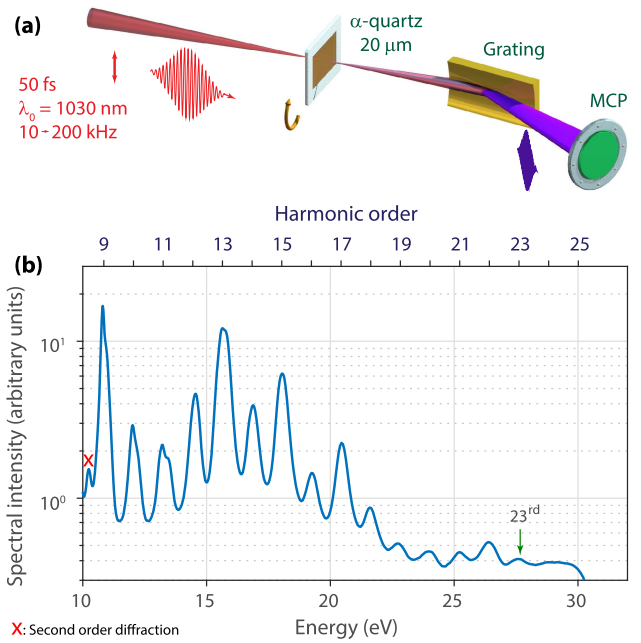

Fig. 1. High-harmonic generation from α–quartz using fiber amplifier laser pulses at 1030 nm center wavelength. (a) Experimental setup, including the solid target and the extreme-ultraviolet spectrometer. (b) Measured spectrum generated from crystalline α–quartz at a 10 kHz repetition rate. The incident pulse energy is 30 μJ. Clear even and odd harmonics can be seen up to 27 eV (23rd harmonic order).

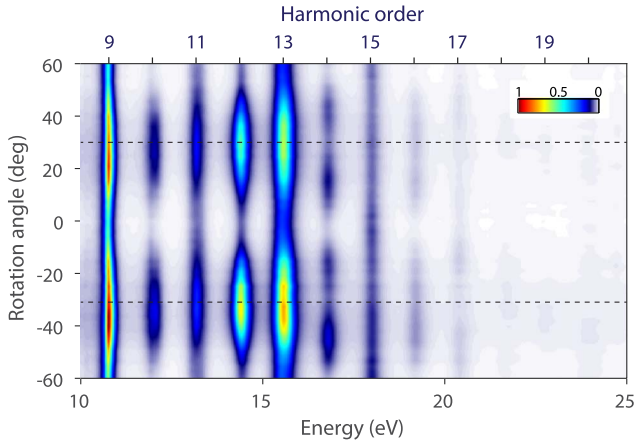

Fig. 2. Six-fold symmetry of α–quartz seen with a rotation measurement. Integrated spectral intensity of HHG from α–quartz as a function of the rotation angle of the crystal with respect to the normal incident laser pulses. The dashed black lines indicate the angles at which the intensity of the radiation is maximized.

coupled to a phosphor screen. The sample is placed on the designated object plane of the grating to achieve optimal spectral resolution and maximal recorded spectral intensity. The crystal rotation stage allows us to record the spectral intensity of the HHG emission as a function of the crystal orientation.

Figure 1(b) shows the typical spectral intensity recorded from the interaction of the linearly polarized laser pulses with the α–quartz sample. Using the measured incident pulse energy, the estimated peak electric field inside the sample is ~0.6 V/Å (with an error of ±10%). The measured spectrum shows both the broadband EUV emission covering a total bandwidth (the spectral extent over which there are photons) of ~20 eV with the emission of both even and odd harmonics. The even-harmonic emission is the manifestation of broken inversion symmetry, which has also been observed in ZnO [5,24]. The broad bandwidth of this radiation will make HHG sources such as the present one a great alternative, potentially replacing EUV HHG from gases because of the considerably reduced complexity of the laser source and HHG target.

In the next step, to further characterize our EUV HHG produced from laser pulses at 1030 nm, we record the spectral intensity at different crystal orientations. The results are shown in Fig. 2. While in ZnO the crystal orientation measurement showed a 90° periodicity [5,24], our measurement shows a 60° periodicity. For z-cut α–quartz, the Brillouin zone has six-fold symmetry, similar to GaSe [19], which is a broken inversion symmetry medium where even harmonics can also be generated. Thus, the six-fold symmetry is exactly what we have observed in our measurement. Furthermore, since the emitted EUV HHG spectral intensity depends on the crystal rotation, our results could help in understanding the crystal structure and, ultimately, its electronic properties.

We additionally measure the spectral intensity of different harmonics as a function of the peak electric field strength. In this case, the spectral intensity at a given peak electric field strength is the average of spectral intensities at all crystal orientations normal to the incident laser pulses. Remarkably, in the regime of 1.2 eV excitation corresponding to a 1030 nm wavelength, all harmonics follow very similar scaling laws, as shown in Fig. 3. First-order logarithmic fitting of the recorded data results in first-order coefficients ranging from E^{10}–E^{16} for all harmonics. The fits to two of the harmonic orders are shown in Fig. 3. Taking into account the harmonics in consideration (H9–H15), the fitted coefficients support the highly-nonperturbative picture of HHG from solids, as

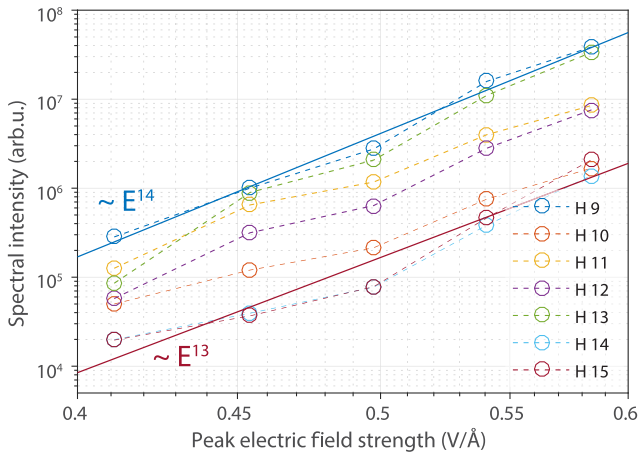

Fig. 3. Scaling of spectral intensity of α–quartz, depending on the peak electric field strength. Integrated spectral intensities of different harmonic orders are illustrated as circles. The dashed lines are guides to the eye. The straight solid lines are first-order logarithmic fits to the intensity scaling data of harmonic 9 (H9) and harmonic 15 (H15). The resultant first-order coefficients are noted next to the lines.

the perturbative scaling would correspond to E^{18}–E^{30}. Nonperturbative scaling has also been reported in previous works [5,7,10,11].

Moreover, we note that the scaling of all the above harmonics does not reach saturation at the highest applied field strength of 0.6 V/Å. Saturation in intensity scaling of HHG from solids is often reported [5,7,8,24]. If the main contribution to the generated EUV harmonics is from intraband excitations, the saturation can be understood from the characteristics of the associated Bessel functions at a high peak electric field [7]. If interband polarization is the main contributor to the EUV harmonics, the saturation can be understood to be a result of significant depletion of electron (hole) populations due to the strong incident electric field. In our case, experimental probing of spectral intensity at electric field strengths higher than 0.6 V/Å is not possible because of crystal damage. Considering that we are using a longer laser pulse and lower photon energy compared to [7], this fact might be attributed to scattering processes and/or electrical breakdown [25]. These might be the same reasons underlying the similarly observed intensity scaling in MoS_2 [10], although more thorough investigations would be needed to clarify this.

In the next step of our experiment, we proceed to quantify how the repetition rate of our laser system affects the generated photon flux per laser shot. An extremely large number of experiments would benefit from the ability to generate EUV HHG at very high repetition rates. Our laser system allows us to change the repetition rate without changing the pulse energy and pulse duration, as verified by our observations. The results of our measurements are shown in Fig. 4. We observe that while the spectra do not change as a function of the repetition rate, Fig. 4(a), there is a slight drop of spectral intensity per laser shot with an increasing repetition rate, Fig. 4(b). However, taking the repetition rate into account, the increase of the total photon flux per second is ~7 times when the repetition rate is changed from 10 to 200 kHz.

To further investigate the slight drop of spectral intensity at high repetition rates, we note that our MCP (double stack in Chevron configuration) and phosphor screen (P-46) has a response time of ~1 ns and ~0.3 μs, respectively. Thus, even when we operate at the highest repetition rate of 200 kHz, the interval between the laser shots, 5 μs, is sufficiently long for the phosphor screen signal to decay back to zero, ready for the next laser shot. Therefore, the flat–field EUV spectrometer did not operate in the saturation regime. Additionally, the time interval between the laser shots, even at 200 kHz, is six orders of magnitude longer than the longest decay time of acoustic phonon modes of quartz [26], which is on the order of a few picoseconds. Therefore, the drop of spectral intensity cannot be explained by microscopic effects, but it could possibly be attributed to macroscopic effects such as thermal heating or relaxation.

Finally, we conclude our experiment by measuring the absolute photon flux generated in our EUV HHG. The MCP and phosphor screen stack is replaced by the aluminum-coated EUV photodiode (OptoDiode AXUVAl100). The photodiode signal is amplified by a custom-built charge amplifier, and its output signal is measured using an oscilloscope. Due to the coated aluminum layer, the photodiode only senses the EUV signal above 15 eV. The slow response time of the photodiode and charge amplifier (~100 μs) enable the measurement

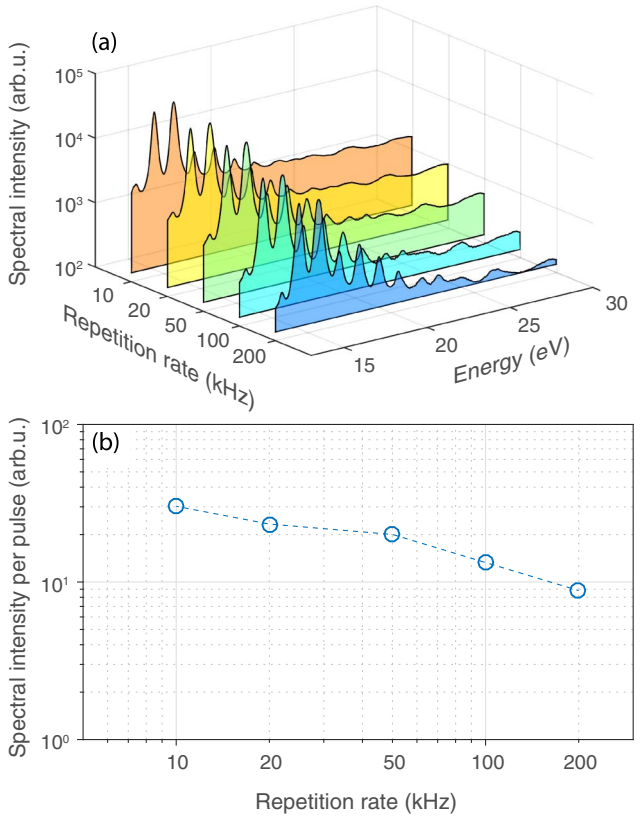

Fig. 4. EUV HHG from solids at high repetition rates. (a) Spectra measured at identical experimental conditions for different repetition rates. (b) Recorded spectral intensity per laser shot as a function of the repetition rate, shown as circles. The dashed lines are guides to the eye.

of the photon flux at 10 kHz or lower repetition rates. In careful calibration of the photon flux taking into account the spectral response of the photodiode, the measured spectrum, the efficiency of the grating, and the response of the MCP, we arrived at a photon flux of ~5×10^5 photon per laser shot at 15.6 eV or 13th harmonic. The estimated absolute error is ~70%. Thus, the current experimental apparatus generates ~5×10^9 photons at 15.6 eV per second at 10 kHz and ~3.5×10^{10} photons per second at the maximum repetition rate of 200 kHz. Compared to optimized gas sources [27,28] our measured photon flux per laser shot is of the same order of magnitude, but our result surpasses them in the number of photons generated per second.

In conclusion, we have demonstrated the creation of EUV radiation through HHG in α–quartz pumped by laser pulses with a duration of 50 fs, pulse energy of 30 μJ, and carrier wavelength of 1030 nm. We have shown that the generated spectral intensity is maintained (same order of magnitude) when we increased the repetition rate from 10 to 200 kHz. At a photon energy of 15.6 eV, our experimental apparatus generates ~3.5×10^{10} photons per second which, to the best of our knowledge, is a record photon flux generated from EUV HHG of solids to date. Future developments may include a fiber amplifier using longer pulse duration [29] and a higher repetition rate [30]. We anticipate that EUV HHG from α–quartz could replace HHG from gases at low photon energies (10–25 eV) in attosecond experiments [31–33]. Furthermore, the high repetition rate of our laser system would

be an ideal candidate for COLTRIMS/coincidence measurements [34,35]. Additionally, following previous work [36] and extending our current work to linearly polarized pulses, the generation of a compact circularly polarized EUV source would be straightforward. Finally, it was suggested in Ref. [19] that, for excitation with ultrashort laser pulses, one can now shape the carrier envelope phase of the generated EUV HHG employing the symmetry of crystals.

Funding. FP7 Ideas: European Research Council (IDEAS-ERC) (307270-ATTOSCOPE); Eidgenössische Technische Hochschule Zürich (ETH) (FEL-11 16-1, FEL-31 15-2); FP7 People: Marie-Curie Actions (PEOPLE) (COFUND).

Acknowledgment. The authors are grateful to Mario Seiler for his contributions to the construction of the experimental apparatus.

REFERENCES

1. P. B. Corkum and F. Krausz, Nat. Phys. **3**, 381 (2007).
2. F. Krausz and M. Ivanov, Rev. Mod. Phys. **81**, 163 (2009).
3. A. McPherson, G. Gibson, H. Jara, U. Johann, T. S. Luk, I. A. McIntyre, K. Boyer, and C. K. Rhodes, J. Opt. Soc. Am. B **4**, 595 (1987).
4. M. Ferray, A. L'Huillier, X. F. Li, L. A. Lompre, G. Mainfray, and C. Manus, J. Phys. B **21**, L31 (1988).
5. S. Ghimire, A. D. DiChiara, E. Sistrunk, P. Agostini, L. F. DiMauro, and D. A. Reis, Nat. Phys. **7**, 138 (2011).
6. O. Schubert, M. Hohenleutner, F. Langer, B. Urbanek, C. Lange, U. Huttner, D. Golde, T. Meier, M. Kira, S. W. Koch, and R. Huber, Nat. Photonics **8**, 119 (2014).
7. T. T. Luu, M. Garg, S. Y. Kruchinin, A. Moulet, M. T. Hassan, and E. Goulielmakis, Nature **521**, 498 (2015).
8. G. Ndabashimiye, S. Ghimire, M. Wu, D. A. Browne, K. J. Schafer, M. B. Gaarde, and D. A. Reis, Nature **534**, 520 (2016).
9. Y. S. You, D. A. Reis, and S. Ghimire, Nat. Phys. **13**, 345 (2017).
10. H. Liu, Y. Li, Y. S. You, S. Ghimire, T. F. Heinz, and D. A. Reis, Nat. Phys. **13**, 262 (2016).
11. G. Vampa, B. G. Ghamsari, S. Siadat Mousavi, T. J. Hammond, A. Olivieri, E. Lisicka-Skrek, A. Y. Naumov, D. M. Villeneuve, A. Staudte, P. Berini, and P. B. Corkum, Nat. Phys. **13**, 659 (2017).
12. N. Yoshikawa, T. Tamaya, and K. Tanaka, Science **356**, 736 (2017).
13. H. Kim, S. Han, Y. W. Kim, S. Kim, and S.-W. Kim, ACS Photonics **4**, 1627 (2017).
14. M. Sivis, M. Taucer, G. Vampa, K. Johnston, A. Staudte, A. Y. Naumov, D. M. Villeneuve, C. Ropers, and P. B. Corkum, Science **357**, 303 (2017).
15. T. Higuchi, M. I. Stockman, and P. Hommelhoff, Phys. Rev. Lett. **113**, 213901 (2014).
16. G. Vampa, T. J. Hammond, N. Thiré, B. E. Schmidt, F. Légaré, C. R. McDonald, T. Brabec, and P. B. Corkum, Nature **522**, 462 (2015).
17. M. Hohenleutner, F. Langer, O. Schubert, M. Knorr, U. Huttner, S. W. Koch, M. Kira, and R. Huber, Nature **523**, 572 (2015).
18. F. Langer, M. Hohenleutner, C. P. Schmid, C. Poellmann, P. Nagler, T. Korn, C. Schüller, M. S. Sherwin, U. Huttner, J. T. Steiner, S. W. Koch, M. Kira, and R. Huber, Nature **533**, 225 (2016).
19. F. Langer, M. Hohenleutner, U. Huttner, S. W. Koch, M. Kira, and R. Huber, Nat. Photonics **11**, 227 (2017).
20. M. Garg, M. Zhan, T. T. Luu, H. Lakhotia, T. Klostermann, A. Guggenmos, and E. Goulielmakis, Nature **538**, 359 (2016).
21. F. Calegari, D. Ayuso, A. Trabattoni, L. Belshaw, S. De Camillis, S. Anumula, F. Frassetto, L. Poletto, A. Palacios, P. Decleva, J. B. Greenwood, F. Martín, and M. Nisoli, Science **346**, 336 (2014).
22. H. J. Wörner, C. A. Arrell, N. Banerji, A. Cannizzo, M. Chergui, A. K. Das, P. Hamm, U. Keller, P. M. Kraus, E. Liberatore, P. Lopez-Tarifa, M. Lucchini, M. Meuwly, C. Milne, J.-E. Moser, U. Rothlisberger, G. Smolentsev, J. Teuscher, J. A. van Bokhoven, and O. Wenger, Struct. Dyn. **4**, 061508 (2017).
23. J. N. Sweetser, D. N. Fittinghoff, and R. Trebino, Opt. Lett. **22**, 519 (1997).
24. S. Gholam-Mirzaei, J. Beetar, and M. Chini, Appl. Phys. Lett. **110**, 061101 (2017).
25. C. Zener, Proc. R. Soc. A **145**, 523 (1934).
26. R. R. Alfano, *Semiconductors Probed by Ultrafast Laser Spectroscopy* (Academic, 1984), Vol. **I**.
27. M. Ito, Y. Kataoka, T. Okamoto, M. Yamashita, and T. Sekikawa, Opt. Express **18**, 6071 (2010).
28. A. von Conta, M. Huppert, and H. J. Wörner, Rev. Sci. Instrum. **87**, 073102 (2016).
29. L. Lavenu, M. Natile, F. Guichard, Y. Zaouter, M. Hanna, E. Mottay, and P. Georges, Opt. Express **25**, 7530 (2017).
30. Y. Liu, W. Li, D. Luo, D. Bai, C. Wang, and H. Zeng, Opt. Express **24**, 10939 (2016).
31. Y. Cheng, M. Chini, X. Wang, A. González-Castrillo, A. Palacios, L. Argenti, F. Martín, and Z. Chang, Phys. Rev. A **94**, 023403 (2016).
32. M. Huppert, I. Jordan, D. Baykusheva, A. von Conta, and H. J. Wörner, Phys. Rev. Lett. **117**, 093001 (2016).
33. L. Gallmann, I. Jordan, H. J. Wörner, L. Castiglioni, M. Hengsberger, J. Osterwalder, C. A. Arrell, M. Chergui, E. Liberatore, U. Rothlisberger, and U. Keller, Struct. Dyn. **4**, 061502 (2017).
34. M. Sabbar, S. Heuser, R. Boge, M. Lucchini, T. Carette, E. Lindroth, L. Gallmann, C. Cirelli, and U. Keller, Phys. Rev. Lett. **115**, 133001 (2015).
35. P. Ranitovic, C. W. Hogle, P. Riviere, A. Palacios, X.-M. Tong, N. Toshima, A. Gonzalez-Castrillo, L. Martin, F. Martin, M. M. Murnane, and H. Kapteyn, Proc. Natl. Acad. Sci. USA **111**, 912 (2014).
36. N. Saito, P. Xia, F. Lu, T. Kanai, J. Itatani, and N. Ishii, Optica **4**, 1333 (2017).